

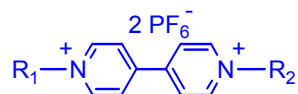
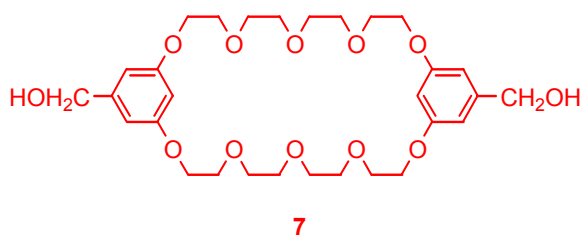
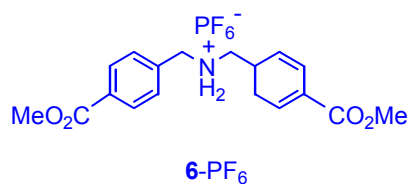
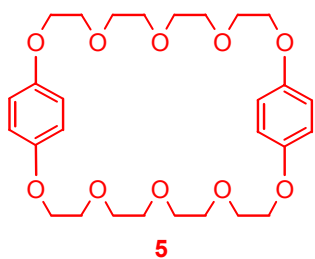
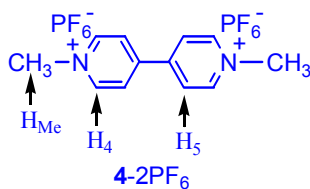
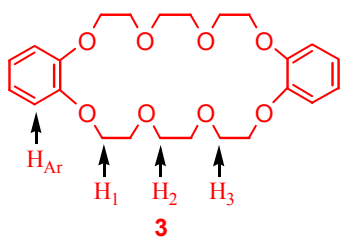
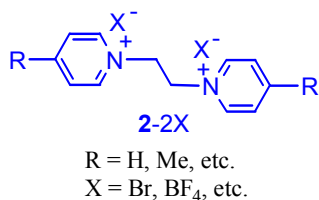
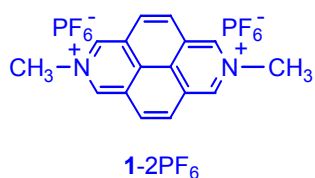
Chapter III

[2]Pseudorotaxanes Based on the Dibenzo-24-Crown-8/Paraquat Recognition Motif

3.1. INTRODUCTION

Paraquat (N,N'-dialkyl-4,4'-bipyridinium) derivatives have been widely used as guests in supramolecular chemistry to construct numerous complexes with large crown ethers, such as bis(*m*-phenylene)-32-crown-10 derivatives and bis(*p*-phenylene)-34-crown-10 derivatives.¹ Dibenzo-24-crown-8 (DB24C8) derivatives, one of the most common families of hosts in supramolecular chemistry, have been used to make a large number of complexes with secondary ammonium salts.^{2,1h} A paraquat-like compound, 2,7-dimethyldiazapyrenium bis(hexafluorophosphate) (**1-2PF₆**),³ and 1,2-bis(pyridinium)ethane derivatives (**2-2X**)⁴ have been reported to form pseudorotaxanes or rotaxanes with DB24C8 (**3**). However, no complexes based on simple paraquat derivatives and DB24C8 derivatives have been successfully constructed up to now. It has been reported that the interaction between dibenzyl paraquat and **3** is negligible,⁵ Here we report some new [2]pseudorotaxanes based on the dibenzo-24-crown-8/paraquat recognition motif. They were characterized by ¹H NMR, mass spectrometry, and X-ray

analysis. We found that the complexation between **3** and the “parent” dimethyl paraquat (**4-2PF₆**) is the strongest among the known systems based on simple crown ethers and organic guests. As shown by X-ray analysis, this pseudorotaxane has a unique 2:1 capsule-like structure in the solid state.

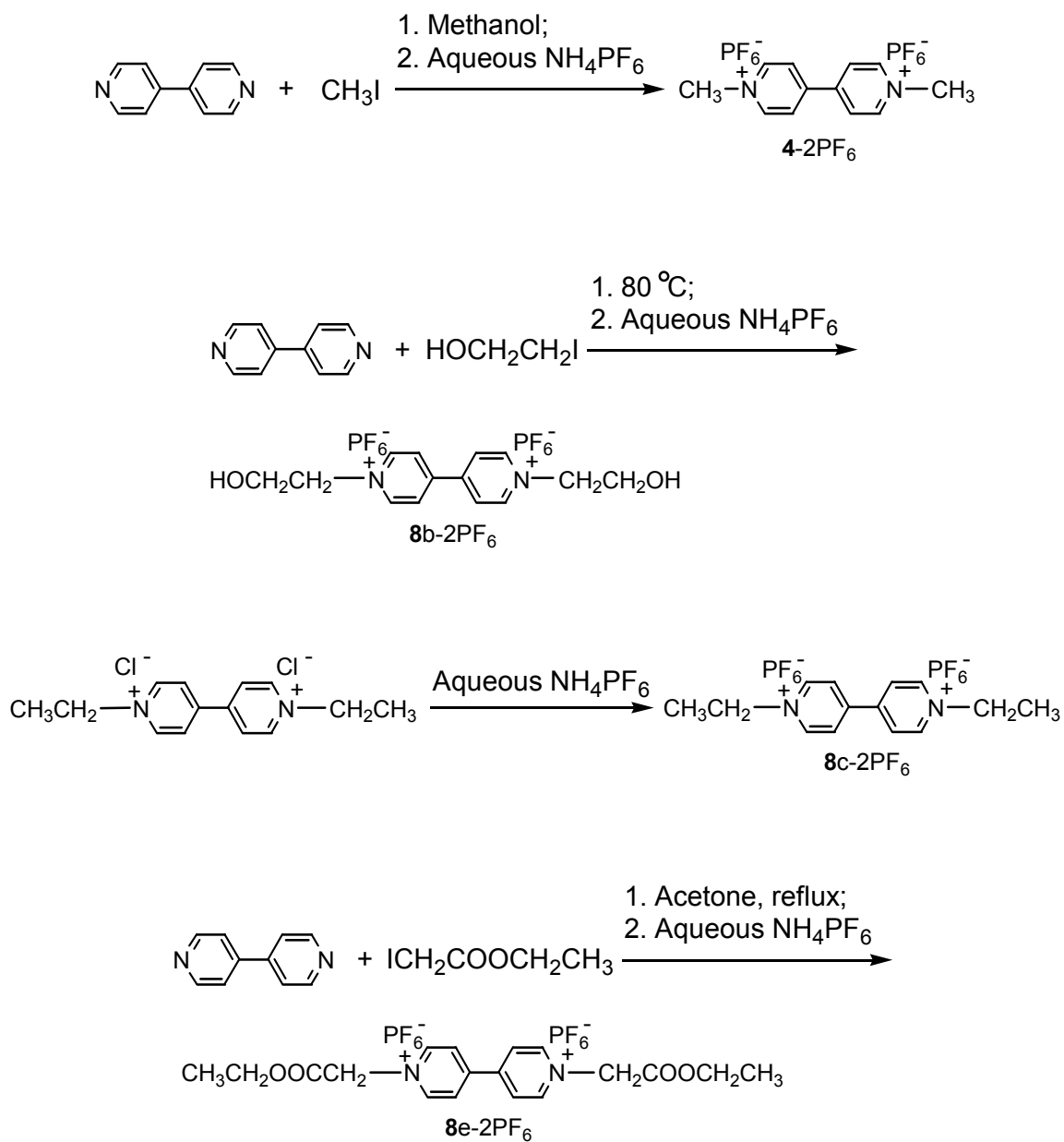


- 8b-2PF₆**: R₁ = R₂ = CH₂CH₂OH
8c-2PF₆: R₁ = R₂ = CH₂CH₃
8d-2PF₆: R₁ = R₂ = CH₂CH₂COOCH₃
8e-2PF₆: R₁ = R₂ = CH₂COOCH₂CH₃

3.2. RESULTS AND DISCUSSIONS

A. Syntheses.

Scheme 1. Syntheses of **4-2PF₆**, **8b-2PF₆**, **8c-2PF₆**, and **8e-2PF₆**.



8a-2PF₆ and **8d-2PF₆** are available from our group. Syntheses of **4-2PF₆**, **8b-2PF₆**, and **8e-2PF₆** started from 4,4'-bipyridine and then needed a counterion exchange process. The synthesis of **8c-2PF₆** involved one step, a counterion exchange process, from a chemical available from our group.

B. Complexation between **3** and **4-2PF₆**.

When **3** was mixed with an equivalent of **4-2PF₆** in CD₃COCD₃, a yellow color was observed immediately due to the charge transfer interactions between the electron-rich aromatic rings of **3** and electron-poor **4-2PF₆**. This solution was characterized by ¹H NMR (Figure 1). Upon complexation H₂ and H₃ in **3** move downfield, while H₁ and H_{Ar} in **3** and H₄, H₅, and H_{Me} in **4-2PF₆** move upfield. A Job plot⁶ (Figure 2) demonstrated that the complex between **3** and **4-2PF₆** was of 1:1 stoichiometry in solution. *K_a* of **3**•**4-2PF₆** calculated based on the proton NMR data (Figures 3 and 4)⁷ was $1.7 (\pm 0.2) \times 10^3$ M⁻¹ at 1.00 mM initial concentrations of **3** and **4-2PF₆**.⁸ This value is the highest among the known systems based on simple crown ethers and organic guests. For examples, the following *K_a*^{298K} values have been reported: **3**•**1-2PF₆**, 840 ± 51 M⁻¹ in CD₃CN;³ **3**•**2-2X**, R = H, X = BF₄, 180 M⁻¹ in CD₃CN;^{4a} **3**•**2-2X**, R = CO₂Et, X = BF₄, 1200 M⁻¹ in CD₃CN;^{4a} **5**•**4-2PF₆**, 730 M⁻¹ in CD₃COCD₃;^{1b} **3**•**6-PF₆**, 1100 M⁻¹ in CD₃CN;^{2c} and **7**•**4-2PF₆**, 570 M⁻¹ in CD₃COCD₃.^{1f}

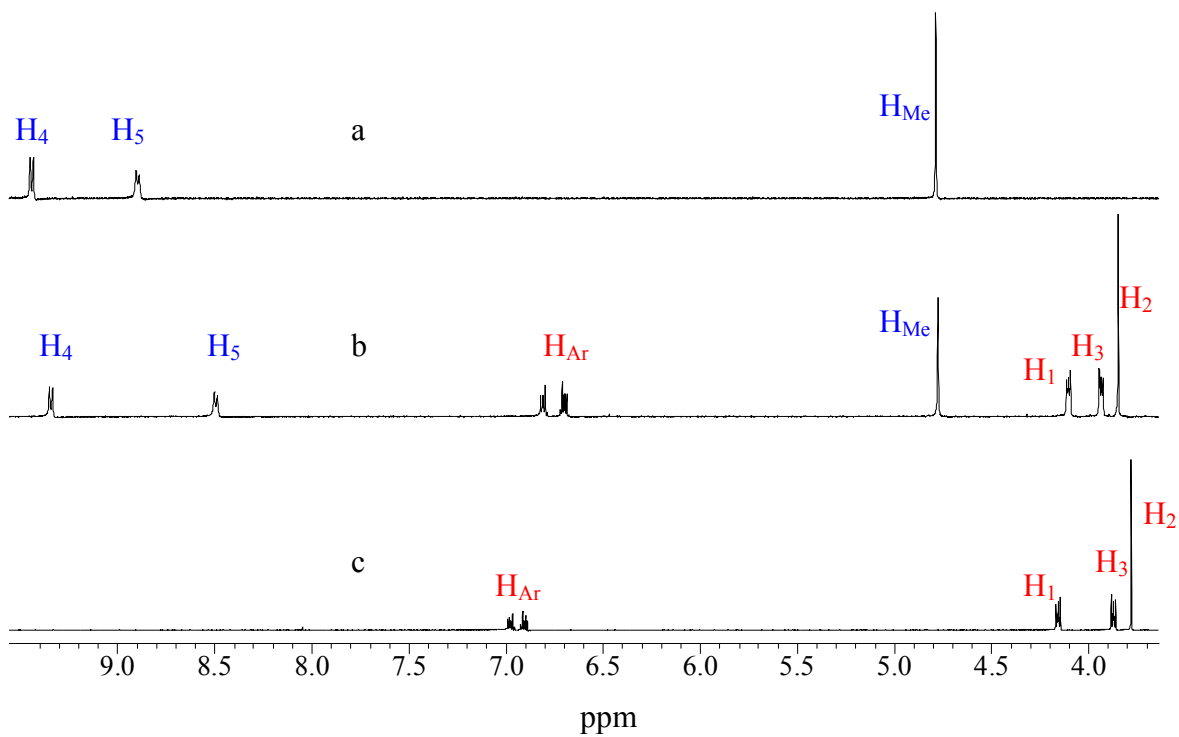


Figure 1. Partial ^1H NMR spectra (400 MHz, CD_3COCD_3 , 298K) of (a) 2.00 mM **4-2PF₆**, (b) 2.00 mM **4-2PF₆** and 2.00 mM **3**, (c) 2.00 mM **3**.

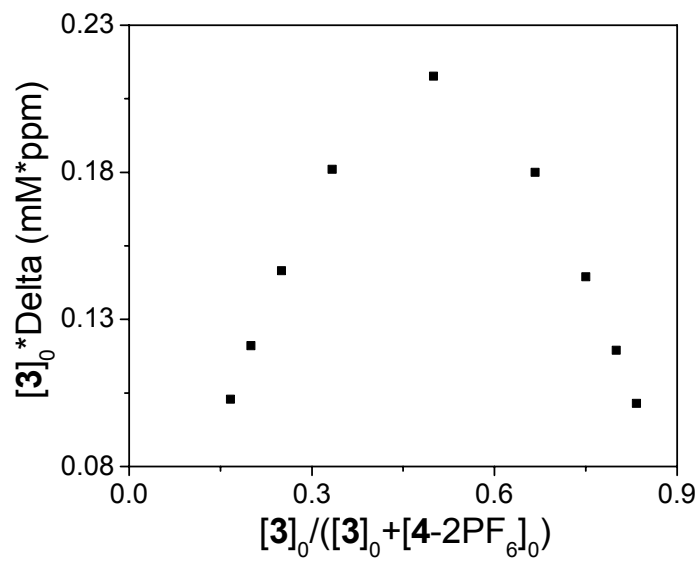


Figure 2. Job plot: the 1:1 stoichiometry of the complex between **3** and 4-2PF₆ in CD₃COCD₃ solution using data for H₂. $[3]_0 + [4-2PF_6]_0 = 6.00$ mM.

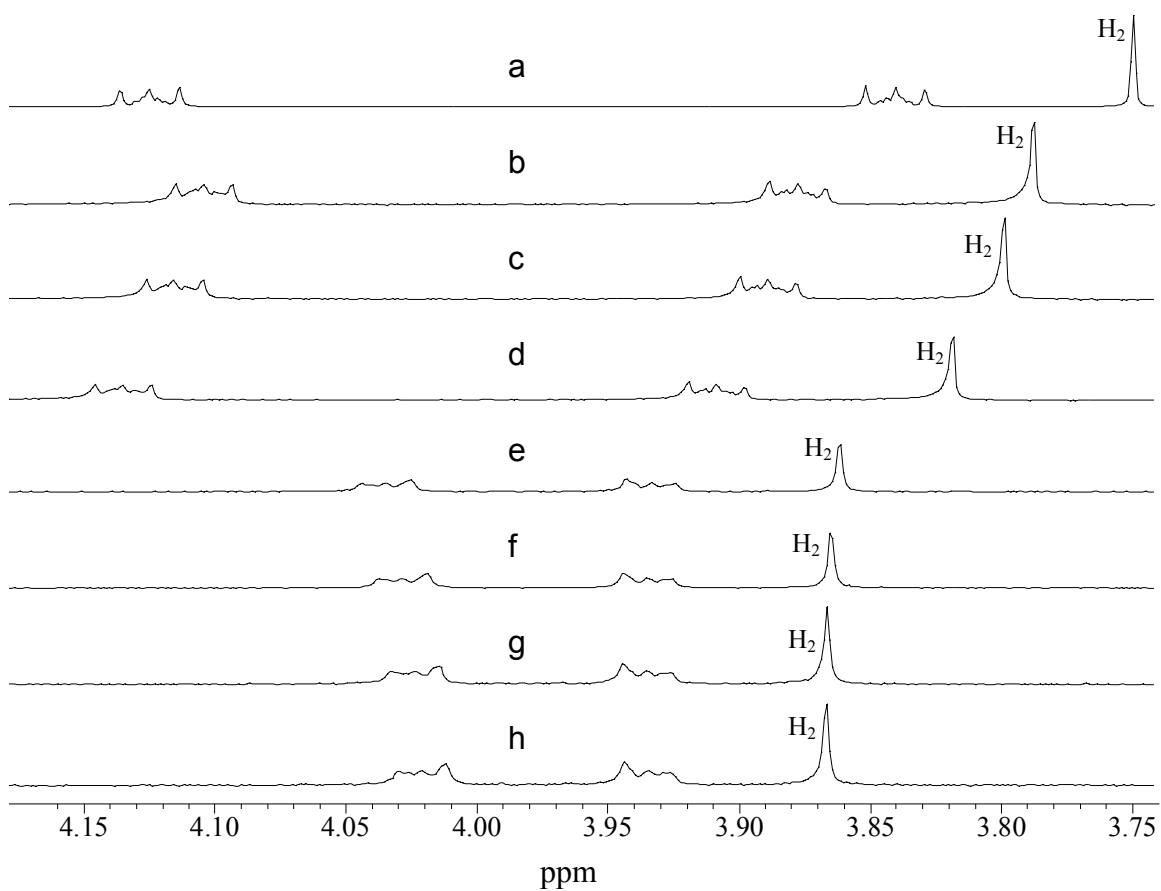


Figure 3. Partial ¹H NMR spectra (400 MHz, acetone-*d*₆, 298K) of (a) 0.500 mM **3**, (b) 0.500 mM **3** and 0.500 mM **4-2PF₆**, (c) 0.500 mM **3** and 0.750 mM **4-2PF₆**, (d) 0.500 mM **3** and 1.50 mM **4-2PF₆**, (e) 0.500 mM **3** and 10.0 mM **4-2PF₆**, (f) 0.500 mM **3** and 20.0 mM **4-2PF₆**, (g) 0.500 mM **3** and 40.0 mM **4-2PF₆**, and (h) 0.500 mM **3** and 60.0 mM **4-2PF₆** showing the chemical shift of H₂ at different concentrations of **4-2PF₆**. For any given solution $\Delta = \delta - \delta_u$; δ_u is defined in spectrum (a).

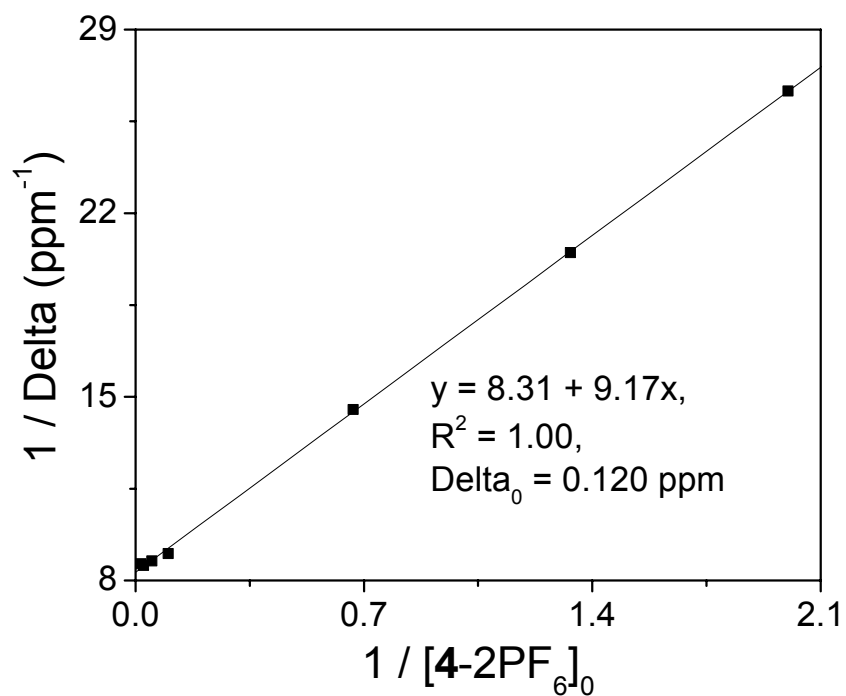


Figure 4. Relationship between $1/\Delta$ and $1/[4-2PF_6]_0$ for the complexation between **3** and **4-2PF₆** in acetone-*d*₆, 22°C. $[3]_0$ and $[4-2PF_6]_0$ are initial concentrations of **3** and **4-2PF₆**. $[3]_0$ is constant at 0.500 mM. This plot is based on NMR data shown in Figure 3.

Low-resolution fast-atom bombardment mass spectrometry (Figure 5, LRFAB-MS, matrix: NBA/PEGNa) of a mixture of **3** and **4-2PF₆** gave direct evidence of the 1:1 complex **3•4-2PF₆**: m/z 779.7 (**3•4-2PF₆** - PF₆)⁹ and 657.4 (**3•4-2PF₆** - 2PF₆ + Na). No peaks related to other stoichiometries were found.

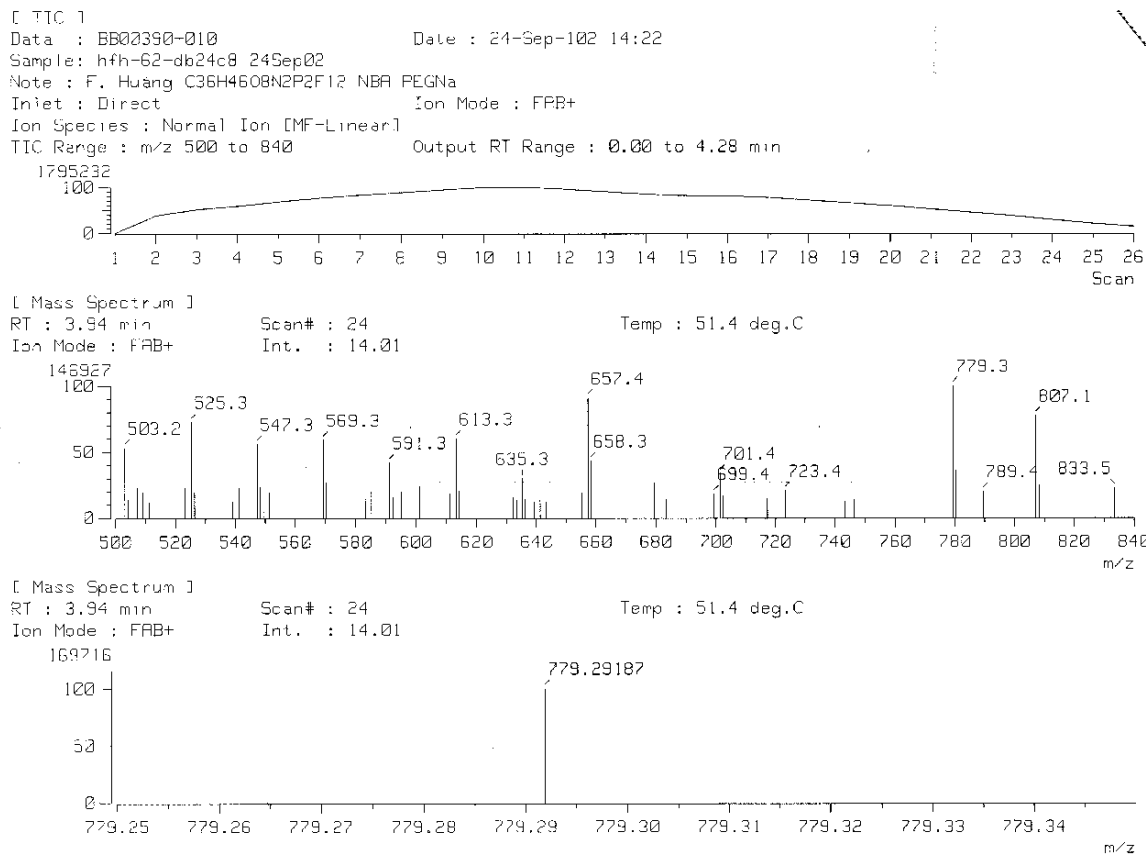


Figure 5. Fast-atom bombardment mass spectrum of a solution of **3** and **4-2PF₆** (1:1 molar ratio).

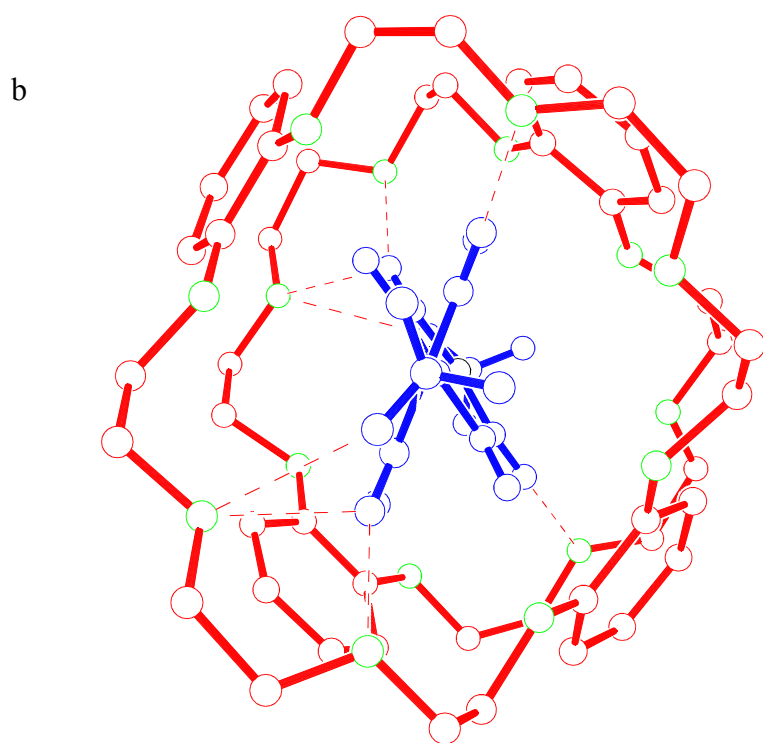
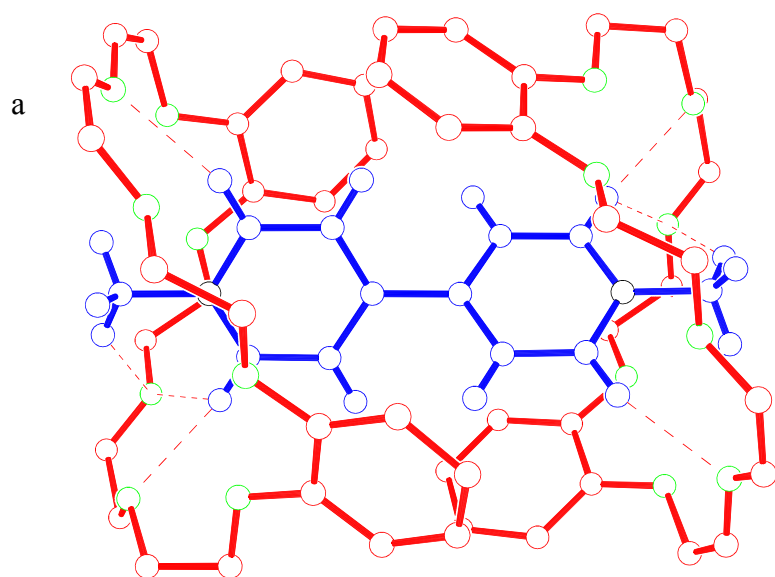
Single crystals of **4-2PF₆** were grown by vapor diffusion of pentane into its acetone solution, while single crystals of the complex were grown from an equimolar acetone solution of **3** and **4-2PF₆** by the same method. In contrast to the 1:1 stoichiometry observed in solution and gaseous states, the crystals of the complex were of 2:1 stoichiometry. In the X-ray crystal structure (Figure 6) of **3•4-2PF₆•3**,¹⁰ two host

molecules are folded to form a structure (Figure 6d) like a capsule, a topic of great current interest in supramolecular chemistry.¹³ A guest molecule resides at the center of the cavity provided by the capsule. The angle between the two pyridinium rings of **4**-2PF₆ changed from 0° (Figure 7)¹⁴ to 54.3° in **3•4**-2PF₆•**3** (Figure 6b). This apparently occurs in order to maximize the N⁺...O interactions.^{4a,1b} This torsion angle is the largest reported for complexes of paraquat derivatives: compare to 11.4° in **7•4**-2PF₆,^{1f} 0° in **5•4**-2PF₆^{1b} and 5.8° in a complex with a cryptand.^{1f} It is impossible to have this kind of torsion in **1**-2PF₆. This results in different orientations of the two crown ether rings observed in **3•4**-2PF₆•**3** and **3•1**-2PF₆•**3**. In the present complex a capsular structure results from an opposing, head-to-head orientation of the hosts, both of whose benzo rings interact with the guest (Figure 6d). The complex with the diazapyrenium salt features a head-to-tail structure of the two host species in which one pair of benzo rings does not interact with the guest (Figure 6e).³ Sixteen N⁺...O interactions (Figure 5c) exist in **3•4**-2PF₆•**3** with distances ranging from 3.082 to 3.841 Å. On each side of the complex, a pyridinium nitrogen atom is nicely positioned at the center of eight catechol oxygens of a crown ether molecule. The average N⁺...O interaction distance in this structure is 3.549 Å, much shorter than that (4.18 Å) in a complex^{4a} between **3** and **2**-2X (R = CO₂Et, X = BF₄), in which four N⁺...O interactions were found.

The complex **3•4**-2PF₆•**3** is also stabilized by eight hydrogen bonds (Figure 6). Six hydrogen bonds involve the four α-protons on the pyridinium rings of **4**-2PF₆ and four ethyleneoxy oxygens of **3**. The other two hydrogen bonds are between methyl protons and ethyleneoxy oxygens. H-bonding of the methyl protons of paraquat is not common in paraquat-based complexes. It exists in the complex of **4**-2PF₆ with **5**,^{1b} but

does not exist in complexes of **4**-2PF₆ with **7**,^{1f} a cryptand,^{1f} nor a supramolecular cryptand.^{1g}

Further stabilization arises from four face-to-face π -stacking interactions between the electron-rich phenylene rings of **3** and electron-poor pyridinium rings of **4**-2PF₆ with centroid-centroid distances of 4.381 and 3.866 Å and dihedral angles of 27.8° and 17.2°. The face-to-face π -stacking interactions appear to be relatively weak in view of the large centroid-centroid distances and dihedral angles.^{1f-g}



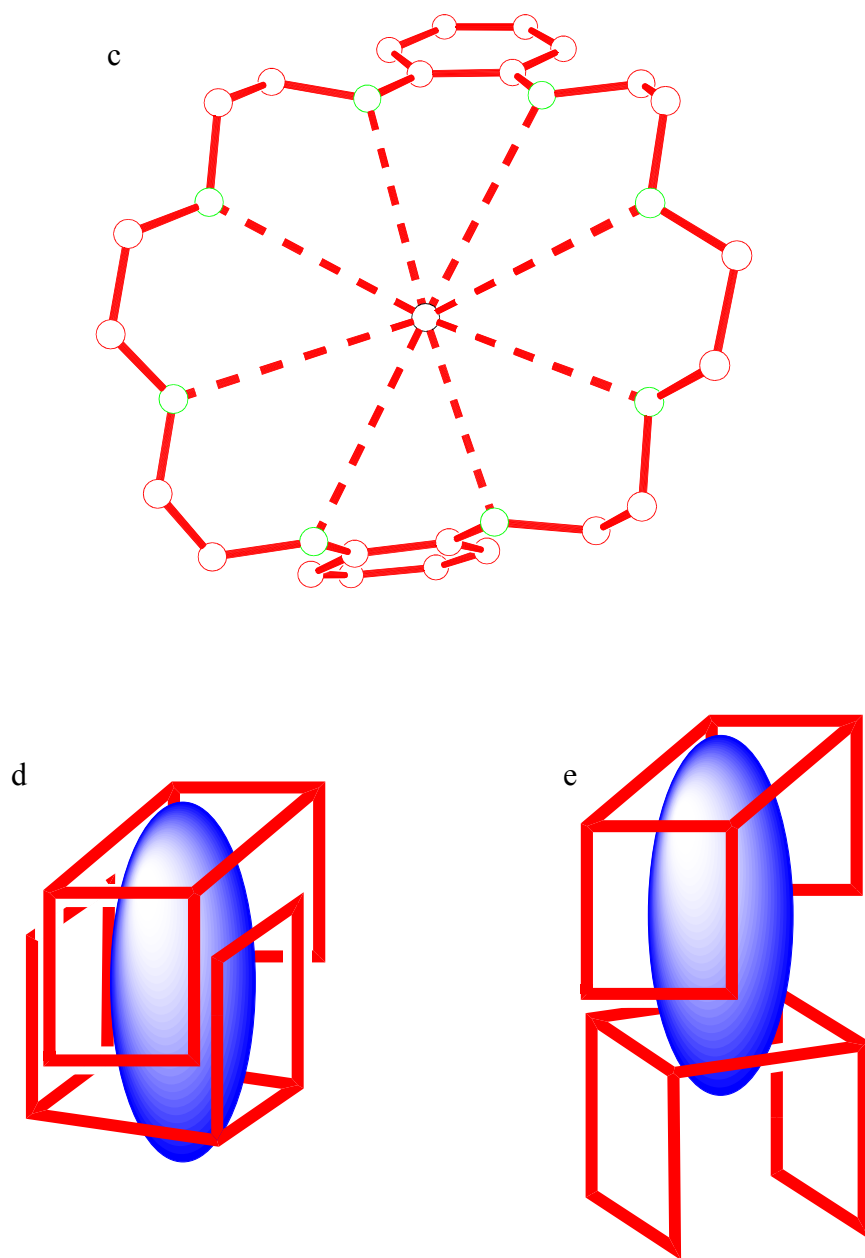


Figure 6. Two views of the solid-state structure of $3\bullet 4\text{-}2\text{PF}_6\bullet 3$ as determined by X-ray crystallography (a and b), a partial view of $3\bullet 4\text{-}2\text{PF}_6\bullet 3$ showing 8 $\text{N}^+\cdots\text{O}$ interactions at one side of the complex (c), cartoon representation of $3\bullet 4\text{-}2\text{PF}_6\bullet 3$ (d), and cartoon

representation of **3•1-2PF₆•3** (e). Two PF₆ counter ions and hydrogen atoms in **3** have been omitted for clarity. **3** is red, **4-2PF₆** or **1-2PF₆** is blue, oxygens are green, hydrogens are magenta, and nitrogens are black. Dashed and dashed bold lines represent hydrogen bonds and N⁺⋯O interactions respectively. Hydrogen-bond parameters are as follows: C⋯O distances (Å) 3.416, 3.197, 3.188, 3.068; H⋯O distances (Å) 2.625, 2.280, 2.289, 2.445; C-H⋯O angles (deg) 138.0, 161.9, 157.6, 123.0. N⁺⋯O distances (Å): 3.635, 3.841, 3.553, 3.082, 3.375, 3.509, 3.825, 3.570. Face-to-face π -stacking parameters: centroid-centroid distances (Å) 4.381, 3.866; dihedral angles (deg) 27.8, 17.2. The angle and centroid-centroid distance between two pyridinium rings of **4-2PF₆** (deg and Å): 54.3 and 4.251.

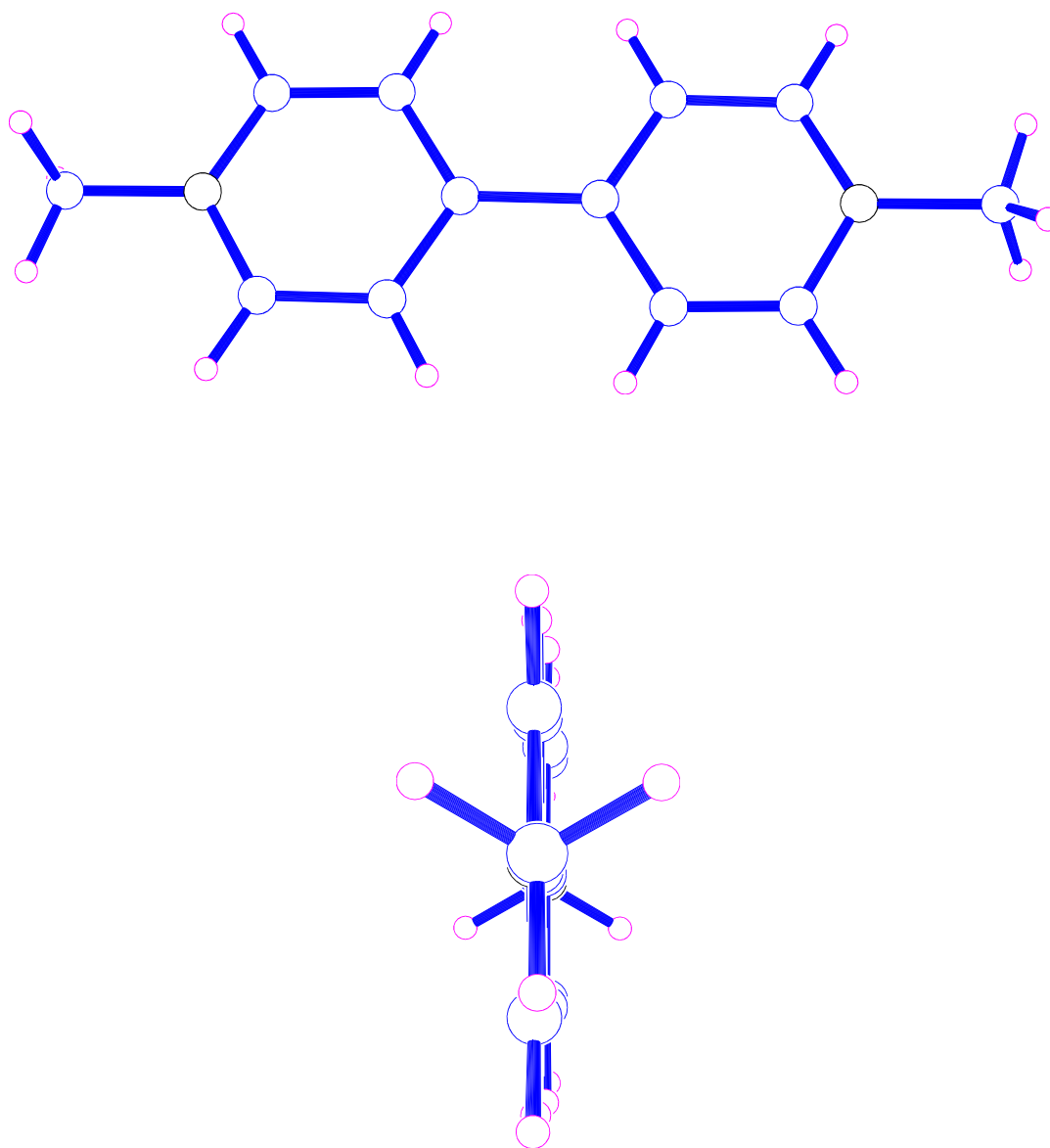


Figure 7. Two views of the solid-state structure of **4-2PF₆** as determined by X-ray crystallography. Two PF₆ counter ions have been omitted for clarity. Hydrogens are magenta, and nitrogens are black. The angle and centroid-centroid distance between two pyridinium rings of **4-2PF₆** (deg and Å): 0 and 4.276.

C. Complexation between **3** and other paraquat derivatives

Here we want to extend this new recognition motif to other paraquat derivatives in order to determine the most important interactions between **3** and paraquat derivatives **8-2PF₆**. A mixture of 1.00 mM **3** and 1.00 mM methyl/hydroxyethyl paraquat (**8a-2PF₆**) in acetone has a pale yellow color due to the charge transfer between electron-rich aromatic rings on **3** and electron-poor pyridinium rings of **8a-2PF₆**. This mixture was characterized by proton NMR (Figure 8). Chemical shifts of pyridinium hydrogens on the guest **8a-2PF₆** and aromatic hydrogens on the host **3** changed. This means that these hydrogens were directly involved in interactions between the host and the guest, such as hydrogen bonding and face-to-face π -stacking interactions. A Job plot (Figure 9) based on proton NMR data of H₂ demonstrated that the complex between **3** and **8a-2PF₆** was of 1:1 stoichiometry in acetone solution. K_a of **3**•**8a-2PF₆** calculated for 1:1 complex using Δ_0 estimated by the Benesi-Hildebrand method based on proton NMR data of H₂ (Figures 10 and 11) was $7.5 (\pm 0.4) \times 10^2 \text{ M}^{-1}$, at 1.00 mM initial concentrations of **3** and **8a-2PF₆**. This is higher than apparent association constants of some well-known complexes, $5.3 (\pm 0.3) \times 10^2 \text{ M}^{-1}$ for **5**•**4-2PF₆**, $5.1 (\pm 0.8) \times 10^2 \text{ M}^{-1}$ for **3**•dibenzylammonium hexafluorophosphate, and $5.5 (\pm 0.3) \times 10^2 \text{ M}^{-1}$ for bis(*m*-phenylene)-32-crown-10•**4-2PF₆**, but it is lower than that ($1.7 (\pm 0.2) \times 10^2 \text{ M}^{-1}$) for **3**•**4-2PF₆**.

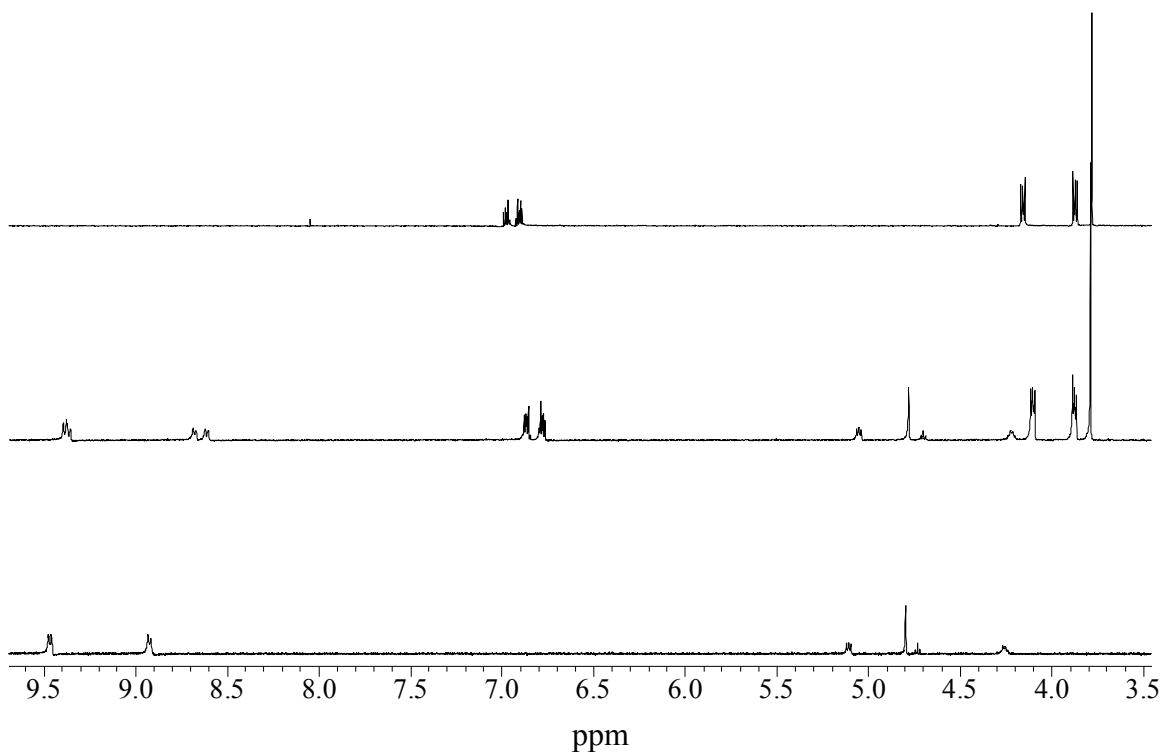


Figure 8. ¹H NMR spectra (400 MHz, CD₃COCD₃, 22 °C) of (a) 1.00 mM **3**, (b) 1.00 mM **3** and 1.00 mM **8a-2PF₆**, (c) 1.00 mM **8a-2PF₆**.

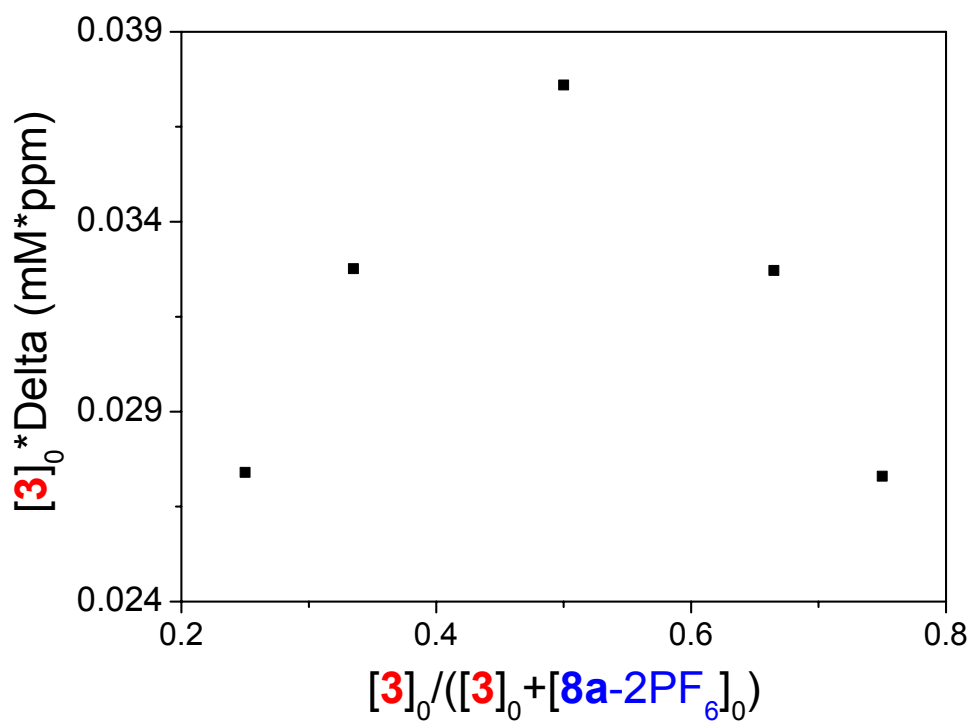


Figure 9. Job plot: the 1:1 stoichiometry of the complex between **3** and **8a-2PF₆** in CD₃COCD₃ solution using data for H₂. $[3]_0 + [8a-2PF_6]_0 = 2.00$ mM.

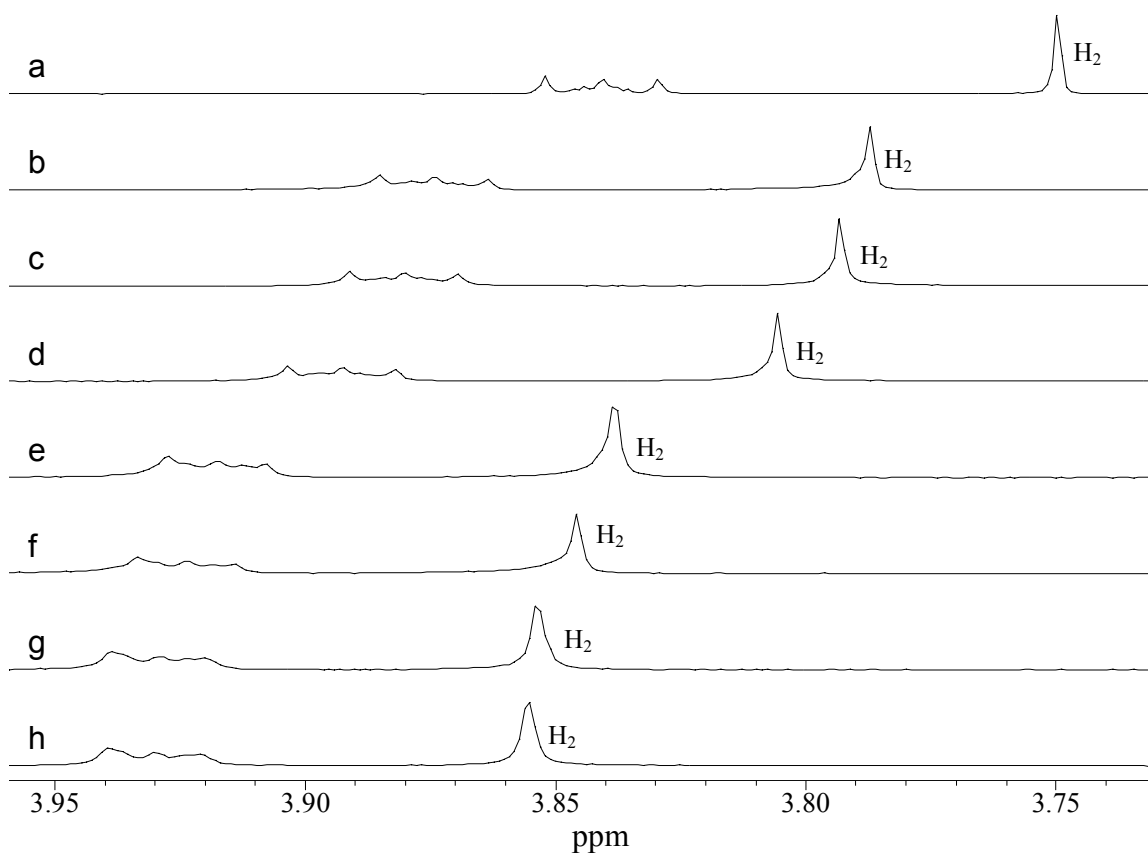


Figure 10. Partial ^1H NMR spectra (400 MHz, acetone- d_6 , 298K) of (a) 1.00 mM **3**, (b) 1.00 mM **3** and 1.00 mM **8a-2PF₆**, (c) 1.00 mM **3** and 1.25 mM **8a-2PF₆**, (d) 1.00 mM **3** and 2.00 mM **8a-2PF₆**, (e) 1.00 mM **3** and 6.00 mM **8a-2PF₆**, (f) 1.00 mM **3** and 11.0 mM **8a-2PF₆**, (g) 1.00 mM **3** and 30.0 mM **8a-2PF₆**, and (h) 1.00 mM **3** and 60.0 mM **8a-2PF₆** showing the chemical shift of H_2 at different concentrations of **8a-2PF₆**. For any given solution $\Delta = \delta - \delta_i$; δ_i is defined in spectrum (a).

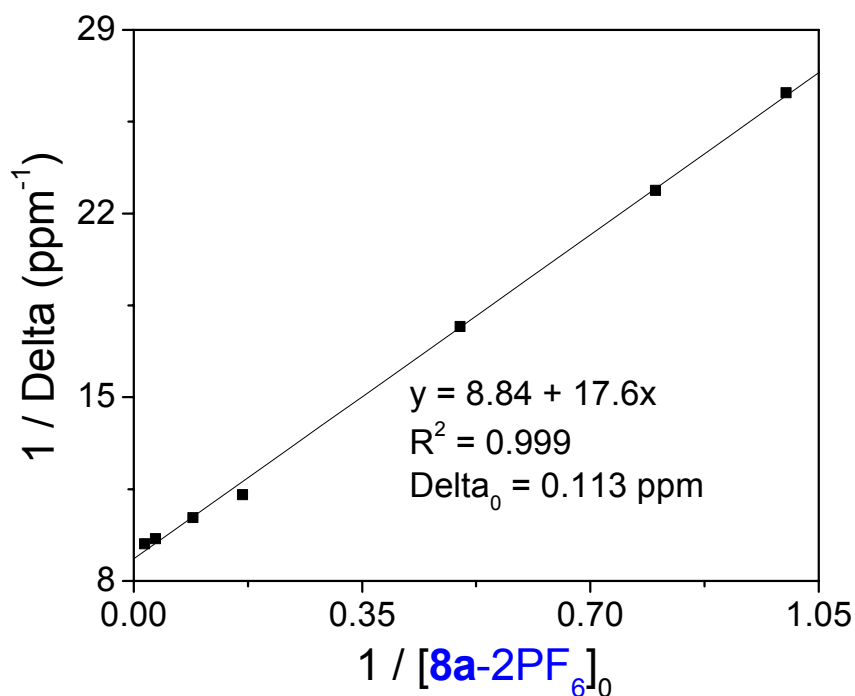


Figure 11. Relationship between $1/\Delta$ and $1/[\mathbf{8a-2PF}_6]_0$ for the complexation between **3** and **8a-2PF₆** in acetone-*d*₆, 22°C. $[\mathbf{3}]_0$ and $[\mathbf{8a-2PF}_6]_0$ are initial concentrations of **3** and **8a-2PF₆**. $[\mathbf{3}]_0$ is constant at 1.00 mM. This plot is based on NMR data shown in Figure 10.

The mixture of 1.00 mM **3** and 1.00 mM **8b-2PF₆** in acetone is colorless. This mixture was characterized by proton NMR (Figure 12). Chemical shifts of all hydrogens on the guest **8b-2PF₆** or on the host **3** did not have obvious changes. This means that the complexation between **3** and **8b-2PF₆** is very weak in acetone. A Job plot (Figure 13) based on proton NMR data for H₂ demonstrated that the complex between **3** and **8b-2PF₆** was of 1:1 stoichiometry in acetone solution. K_a of **3**•**8b-2PF₆** calculated for 1:1 complex using the Benesi-Hildebrand method based on proton NMR data (Figures 14 and 15) was $48 (\pm 5) \text{ M}^{-1}$, at 1.00 mM initial concentrations of **3** and **8b-2PF₆**. This value is very small

compared with the K_a values of **3•4** [$1.7 (\pm 0.2) \times 10^3 \text{ M}^{-1}$] and **3•8a-2PF₆** [$7.5 (\pm 0.4) \times 10^2 \text{ M}^{-1}$].

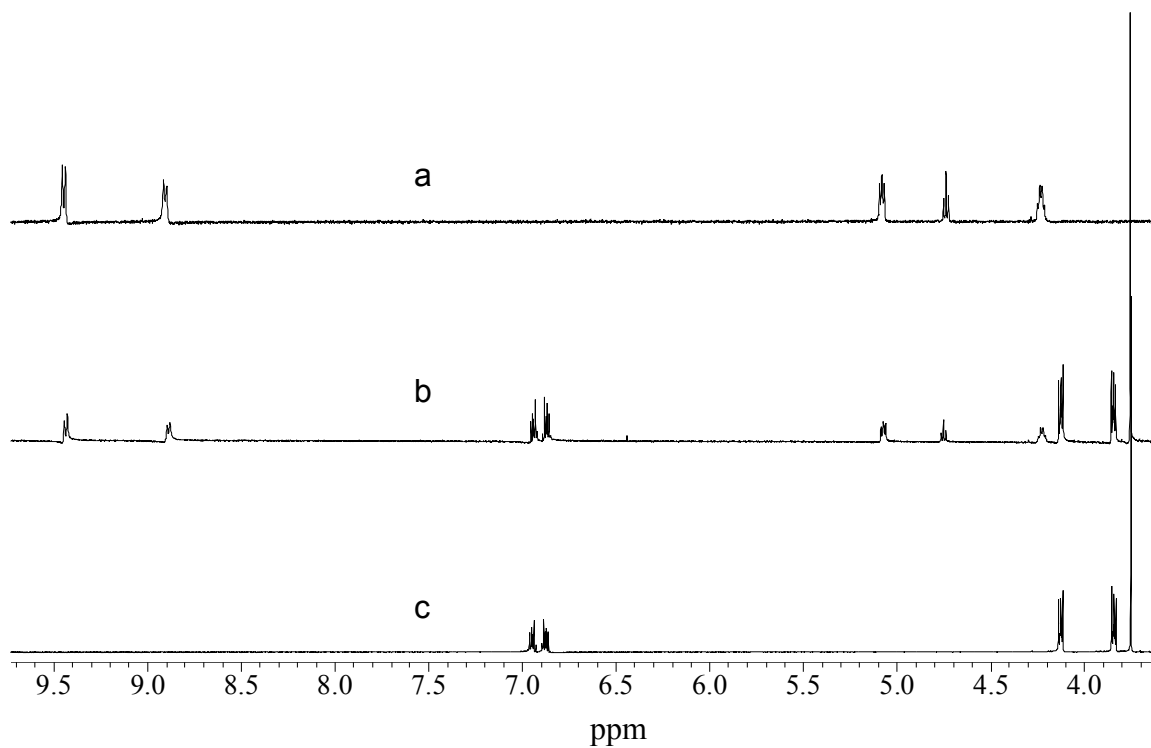


Figure 12. ¹H NMR spectra (400 MHz, CD₃COCD₃, 22 °C) of (a) 1.00 mM **8b-2PF₆**, (b) 1.00 mM **3** and 1.00 mM **8b-2PF₆**, (c) 1.00 mM **3**.

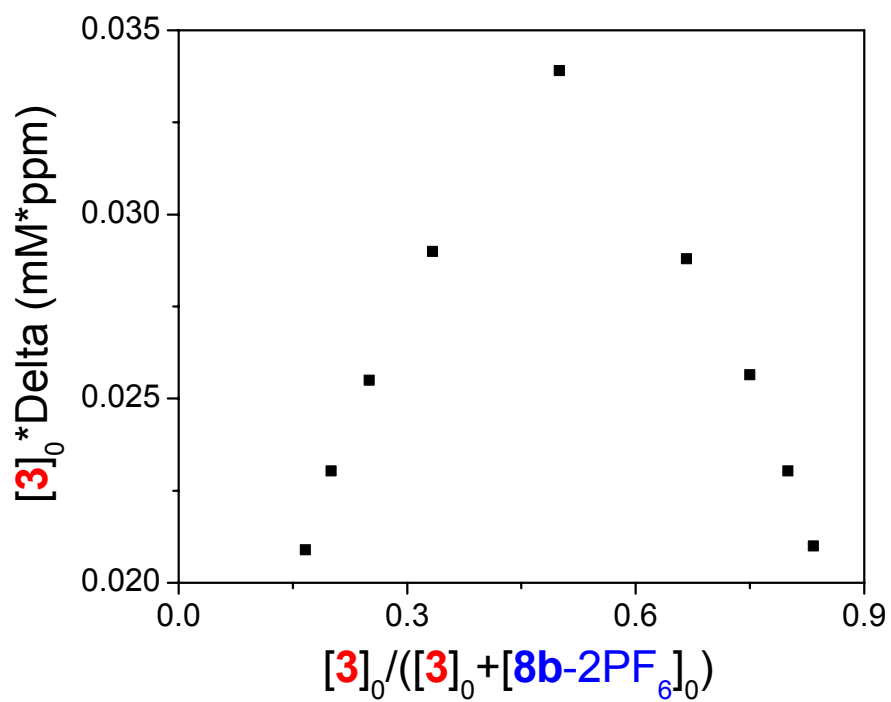


Figure 13. Job plot: the 1:1 stoichiometry of the complex between **3** and **8b-2PF₆** in CD₃COCD₃ solution using data for H₂. $[3]_0 + [8b-2PF_6]_0 = 6.00$ mM.

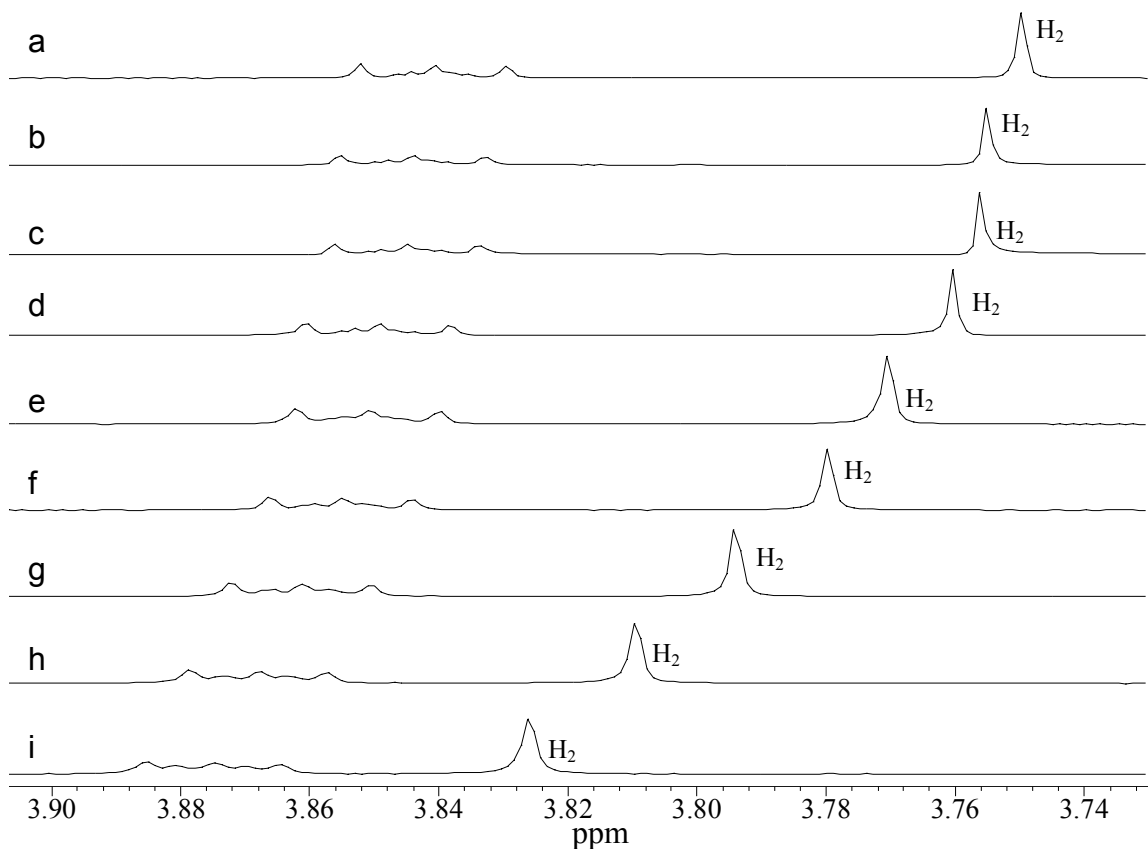


Figure 14. Partial ^1H NMR spectra (400 MHz, acetone- d_6 , 298K) of (a) 1.00 mM **3**, (b) 1.00 mM **3** and 1.00 mM **8b-2PF₆**, (c) 1.00 mM **3** and 1.25 mM **8b-2PF₆**, (d) 1.00 mM **3** and 2.50 mM **8b-2PF₆**, (e) 1.00 mM **3** and 5.00 mM **8b-2PF₆**, (f) 1.00 mM **3** and 10.0 mM **8b-2PF₆**, (g) 1.00 mM **3** and 20.0 mM **8b-2PF₆**, (h) 1.00 mM **3** and 40.0 mM **8b-2PF₆**, and (i) 1.00 mM **3** and 100.0 mM **8b-2PF₆** showing the chemical shift of H_2 at different concentrations of **8b-2PF₆**. For any given solution $\Delta = \delta - \delta_i$; δ_i is defined in spectrum (a).

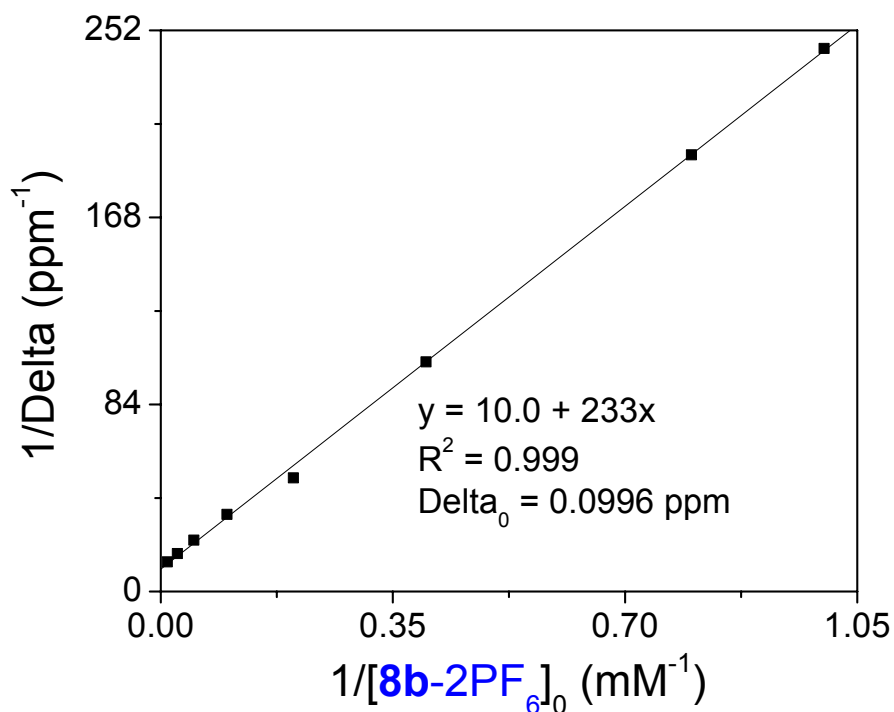


Figure 15. Relationship between $1/\Delta$ and $1/[\mathbf{8b-2PF}_6]_0$ for the complexation between **3** and **8b-2PF₆** in acetone-*d*₆, 22°C. $[\mathbf{3}]_0$ and $[\mathbf{8b-2PF}_6]_0$ are initial concentrations of **3** and **8b-2PF₆**. $[\mathbf{3}]_0$ is constant at 1.00 mM. This plot is based on NMR data shown in Figure 14.

In the same way, the complexes between **3** and **8c-2PF₆** – **8e-2PF₆** were also determined to be of 1:1 stoichiometry in acetone by Job plots. The apparent association constants were also calculated to be $1.2 (\pm 0.1) \times 10^2$, $1.4 (\pm 0.1) \times 10^2$, and $2.5 (\pm 0.3) \times 10^2 \text{ M}^{-1}$ for **3•8c-2PF₆**, **3•8d-2PF₆**, and **3•8e-2PF₆** respectively at 1.00 mM host and guest using the Benesi-Hildebrand method based on proton NMR data of H₂ (Figures 16-18). Comparing these values, we deduce that the substitution of any methyl hydrogen atom on paraquat **8a-2PF₆** will cause K_a decrease, no matter whether the substituents are electron-donating or electron-withdrawing. These values are summarized in Table 1. These values

are understandable. In Chapter 1.13, we already know methyl hydrogens are acidic, so any substitution of these hydrogens will decrease the association constant. Therefore, for K_a , $\mathbf{3\cdot4-2PF_6} > \mathbf{3\cdot8a-2PF_6} > \mathbf{3\cdot8b-2PF_6}$, $\mathbf{3\cdot8c-2PF_6}$, $\mathbf{3\cdot8d-2PF_6}$, and $\mathbf{3\cdot8e-2PF_6}$. Furthermore we saw that for K_a , $\mathbf{3\cdot8e-2PF_6} > \mathbf{3\cdot8d-2PF_6} > \mathbf{3\cdot8c-2PF_6} > \mathbf{3\cdot8b-2PF_6}$. Obviously this happened due to the electron-withdrawing ability of substituent groups: $\text{COOCH}_2\text{CH}_3 > \text{CH}_2\text{COOCH}_3 \approx \text{CH}_2\text{CH}_3 > \text{CH}_2\text{CH}_2\text{OH}$ based on comparisons of Hammett σ values of $\text{COOCH}_2\text{CH}_3$, $\text{CH}_2\text{COOCH}_3$, CH_2CH_3 , and CH_2OH .¹⁸

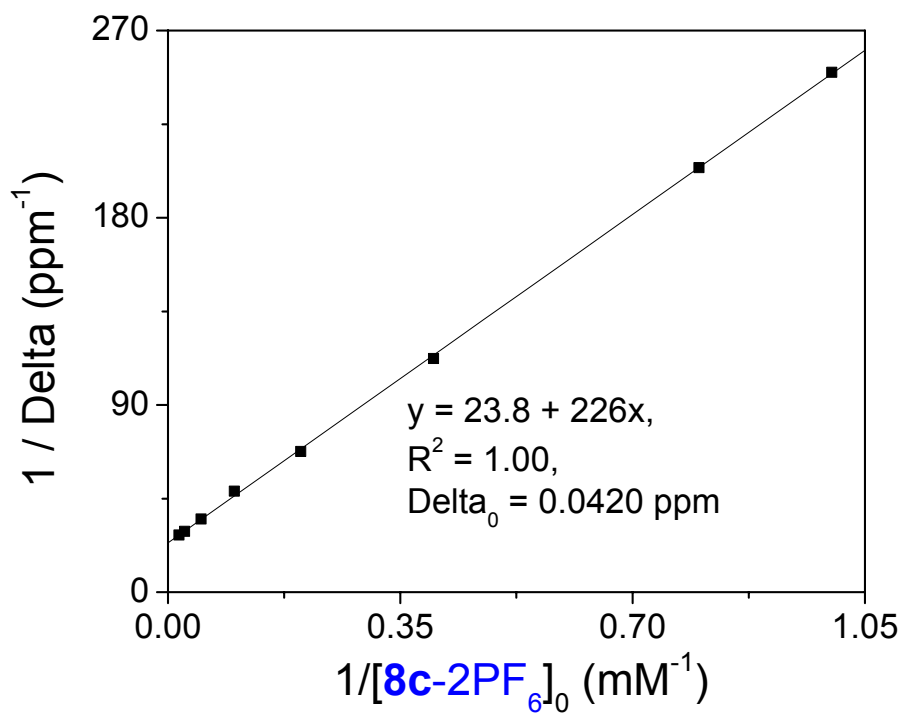


Figure 16. Relationship between $1/\Delta$ and $1/[\mathbf{8c-2PF}_6]_0$ for the complexation between **3** and **8c-2PF₆** in acetone-*d*₆, 22°C. $[\mathbf{3}]_0$ and $[\mathbf{8c-2PF}_6]_0$ are initial concentrations of **3** and **8c-2PF₆**. $[\mathbf{3}]_0$ is constant at 1.00 mM.

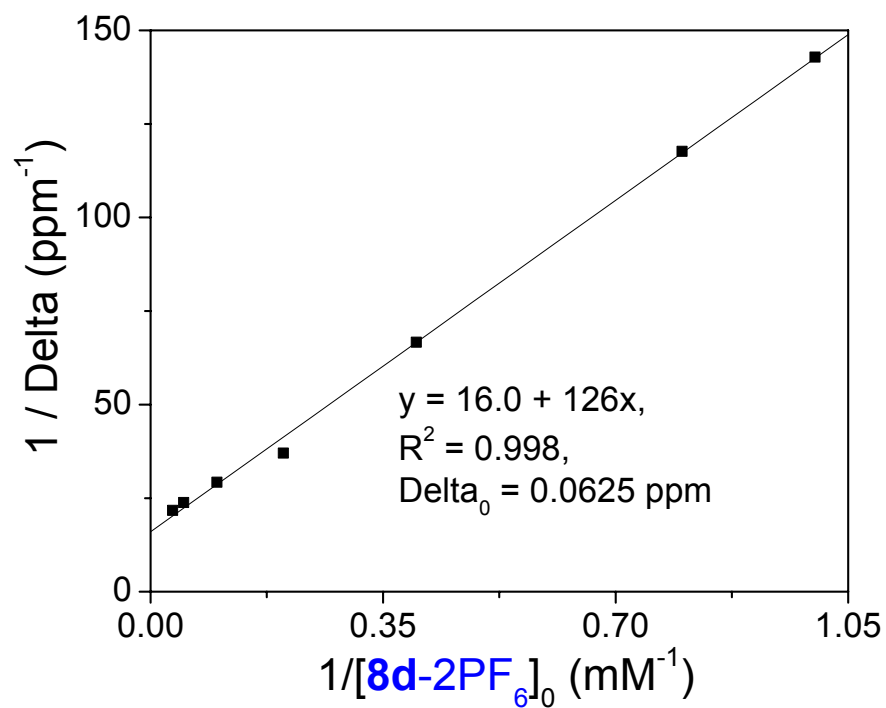


Figure 17. Relationship between $1/\Delta$ and $1/[\mathbf{8d-2PF}_6]_0$ for the complexation between **3** and **8d-2PF₆** in acetone-*d*₆, 22°C. $[\mathbf{3}]_0$ and $[\mathbf{8d-2PF}_6]_0$ are initial concentrations of **3** and **8d-2PF₆**. $[\mathbf{3}]_0$ is constant at 1.00 mM.

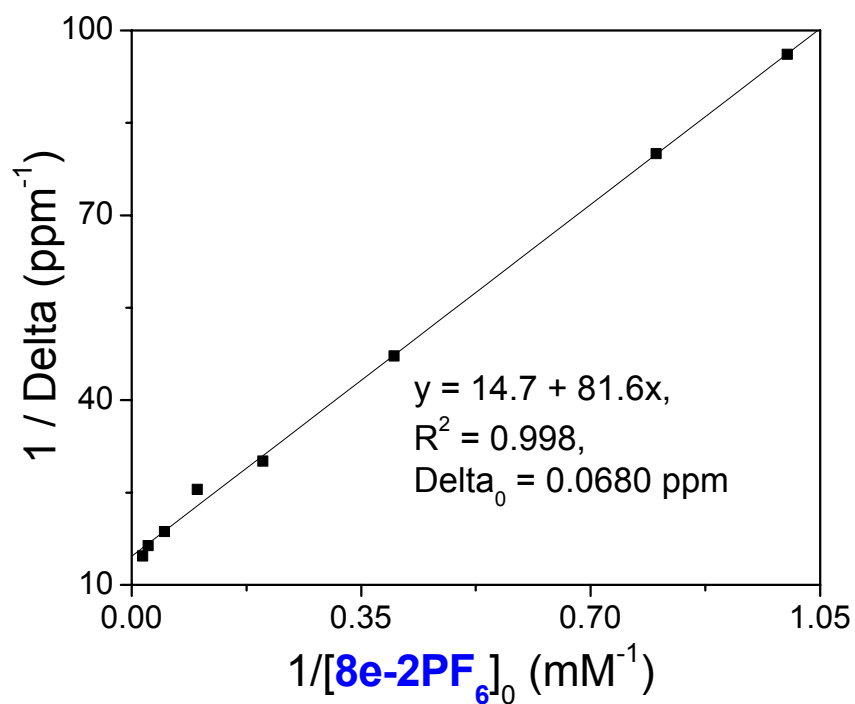
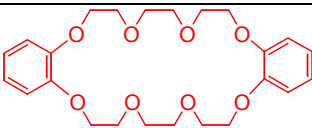
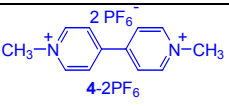
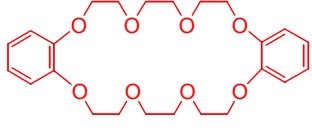
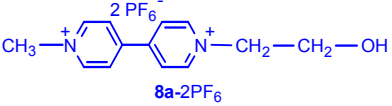
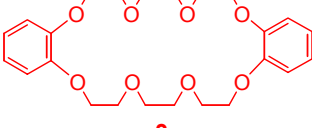
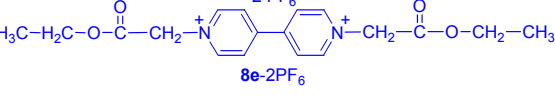
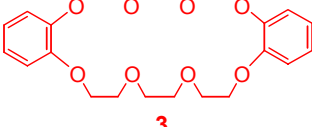
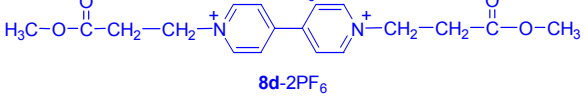
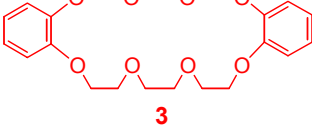
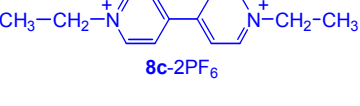
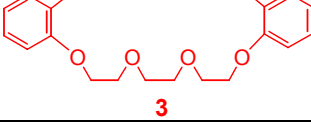
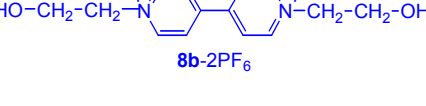


Figure 18. Relationship between $1/\Delta$ and $1/[\mathbf{8e-2PF}_6]_0$ for the complexation between **3** and **8e-2PF₆** in acetone-*d*₆, 22°C. $[\mathbf{3}]_0$ and $[\mathbf{8e-2PF}_6]_0$ are initial concentrations of **3** and **8e-2PF₆**. $[\mathbf{3}]_0$ is constant at 1.00 mM.

Table 1. K_a values for [2]pseudorotaxanes based on dibenzo-24-crown-8 and paraquat derivatives.

Host	Guest	K_a^* (M^{-1})
 3	 4-2PF₆	$1.7 (\pm 0.2) \times 10^3$
 3	 8a-2PF₆	$7.5 (\pm 0.4) \times 10^2$
 3	 8e-2PF₆	$2.5 (\pm 0.3) \times 10^2$
 3	 8d-2PF₆	$1.4 (\pm 0.1) \times 10^2$
 3	 8c-2PF₆	$1.2 (\pm 0.1) \times 10^2$
 3	 8b-2PF₆	$48 (\pm 5)$

*All values are at 1.00 mM host and 1.00 mM guest in acetone.

Low-resolution fast-atom bombardment mass spectrometry (Figure 6, LRFAB-MS, matrix: NBA/PEGNa) of a mixture of **3** and **8b**-2PF₆ gave direct evidence of the 1:1 complex **3**•**8b**-2PF₆: m/z 839.79 (**3**•**8b**-2PF₆ - PF₆)¹⁷. No peaks related to other stoichiometries were found.

3.3. CONCLUSIONS

Thus, a series of new [2]pseudorotaxanes based on the dibenzo-24-crown-8/paraquat recognition motif were prepared and characterized. In the solid state **3**•**4**-2PF₆•**3** was stabilized by N⁺...O interactions, C-H...O hydrogen bonding, and face-to-face π -stacking interactions. Because methyl protons of paraquat are involved in hydrogen bonding to the host, the substitution of any methyl hydrogen atom on paraquat causes K_a to decrease. The electron-withdrawing ability of the substituting group has important influence on the complexation between dibenzo-24-crown-8 and paraquat derivatives.

3.4. ACKNOWLEDGEMENTS

The authors gratefully acknowledge financial support by the National Science Foundation (DMR0097126, HWG).

3.5. EXPERIMENTAL

DB24C8 was purchased from Aldrich and used as received. **8a-2PF₆**¹⁹ and **8d-2PF₆**²² were prepared by known methods.

The 400 MHz ¹H NMR spectra were recorded on a Varian Inova or Varian 400 MHz Instrument.

For the 1:1 complexes between **DB24C8** and paraquat derivatives, fast exchange systems, ¹H NMR characterizations were done on solutions with constant [host]₀ (**DB24C8**) and [guest]₀ (paraquat derivatives) was varied from one to fifty times [host]₀. Based on these NMR data, $\Delta\theta$, the difference in δ values for protons of the host or guest in the uncomplexed and fully complexed species, was calculated by using the Benesi-Hildebrand method.⁷ The complexed host and guest concentrations are represented by [host]_c or [guest]_c, while [host]_{uc} and [guest]_{uc} represent the uncomplexed host and guest concentrations. Then $[\text{host}]_c = [\text{guest}]_c = (\Delta/\Delta\theta)[\text{host}]_0$, $[\text{host}]_{uc} = (1 - \Delta/\Delta\theta)[\text{host}]_0$, $[\text{guest}]_{uc} = [\text{guest}]_0 - [\text{guest}]_c$ and $K_a = [\text{host}]_c / \{[\text{host}]_{uc} [\text{guest}]_{uc}\}$.

N,N'-dimethyl-4,4'-bipyridinium bis(hexafluorophosphate) (4-2PF₆) To a 250 mL 1-necked round bottom flask equipped with a magnetic stirrer and a condenser were added 4, 4'-bipyridyl (10.0 g, 64.2 mmol) and methanol (80 ml) and the solution was warmed to 40 °C. To this solution was added a solution of methyl iodide (21.6 g, 152.4 mmol) in methanol (10 mL) dropwise and the reaction mixture was vigorously stirred under reflux for 24 hours. The reaction mixture was cooled to 0 °C and the suspended materials were filtered to give a solid. The solid was dissolved in 100 mL deionized water. To this aqueous solution was added ammonium hexafluorophosphate until no further precipitation was observed. The precipitate was filtered and recrystallized from deionized water to afford the desired product as small white crystals, 24.4 g (80%). mp 312-313 °C;

no reported values could be found from Scifinder and Beilstein. ^1H NMR (400 MHz, acetone- d_6 , 22 °C) δ 9.46 (d, J = 6.4 Hz, 4H), 8.92 (d, J = 6.4 Hz, 4H), 4.80 (s, 6H).

N,N'-bis(β -hydroxyethyl)-4,4'-bipyridinium bis(hexafluorophosphate) (8b-2PF₆) To 2-iodoethanol (58.0 g, 337 mmol) in a 250 mL 1-necked flask, 4, 4'-bipyridyl (5.65 g, 36 mmol) was added. The flask was immersed in an oil bath at a temperature of 80 °C. The mixture was magnetically stirred under nitrogen for 40 hours. The unreacted 2-iodoethanol was recovered by filtration. The filtrate was added into a 300 mL beaker. NH₄PF₆ (9.65 g, 92 mmol) dissolved in a 100 mL water was added into the filtrate. Precipitate was observed immediately. The mixture was stirred for 30 minutes and filtered. The resultant solid was recrystallized in water 3 times to produce **8b-2PF₆** as white crystals, 15.76 g (81%): mp 202-203 °C; reported: 203-204 °C.²² ^1H NMR (400 MHz, acetone- d_6 , 22 °C) δ 9.44 (d, J = 7.0 Hz, 4H), 8.90 (d, J = 7.0 Hz, 4H), 5.08 (t, J = 5.0 Hz, 4H), 4.74 (t, J = 5.0 Hz, 4H), 4.23 (q, J = 4.6 Hz, 2H).

N,N'-diethyl-4,4'-bipyridinium bis(hexafluorophosphate) (8c-2PF₆) 1.50 g N,N'-diethyl-4,4'-bipyridinium dichloride was dissolved in 65 mL deionized water. Excess NH₄PF₆ was added into this solution until no more precipitate formed. The resultant mixture was filtered to afford a white solid. This white solid was recrystallized in deionized water two times to give pure **8c-2PF₆**, white crystals, 1.19 g (86%). mp 237-238 °C; reported: 236 °C.²¹ ^1H NMR (400 MHz, acetone- d_6 , 22 °C) δ (ppm): 9.53 (d, J = 6.8 Hz, 4H), 8.92 (d, J = 6.8 Hz, 4H), 5.06 (q, J = 7.5 Hz, 4H), 1.85 (t, J = 7.5 Hz, 6H).

N,N'-bis(ethoxycarbonylmethyl)-4,4'-bipyridinium bis(hexafluorophosphate) (8e-2PF₆) To a 50 mL three-necked round bottom flask equipped with a magnetic stirrer and a condenser were added 5.00 g (23.4 mmol) iodoacetic acid ethyl ester and 5 mL acetone. To this solution was added a solution of 4,4'-bipyridine (1.41 g, 9.03 mmol) in 20 mL acetone and the mixture was stirred at reflux for 24 hours. The reaction mixture was cooled to 0 °C and the precipitate was filtered and boiled in CHCl₃. The suspended materials were filtered to give a solid. This solid was dissolved in 100 mL deionized water. To this solution was added NH₄PF₆ until no further precipitation was observed. The precipitate was filtered and recrystallized from water three times to afford the desired product, **8e-2PF₆**, 4.59 g (82%). mp 241-242 °C. ¹H NMR (400 MHz, acetone-*d*₆, 22 °C) δ(ppm): 9.49 (d, *J* = 7.4 Hz, 4H), 9.02 (d, *J* = 7.4 Hz, 4H), 5.99 (s, 4H), 4.34 (q, *J* = 7.5 Hz, 4H), 1.31 (t, *J* = 7.5 Hz, 6H). Anal. calcd for C₁₈H₂₂N₂O₄P₂F₁₂: C, 34.83; H, 3.58; N, 4.52. Found: C, 35.02; H, 3.54; N, 4.53.

Keywords: pseudorotaxane, dibenzo-24-crown-8, paraquat, complex, crown ether

REFERENCES

1. a) B. L. Allwood, H. Shahriari-Zavareh, J. F. Stoddart, D. J. Williams, *J. Chem. Soc., Chem. Commun.* **1987**, 1058-1061; b) B. L. Allwood, N. Spencer, H. Shahriari-Zavareh, J. F. Stoddart, D. J. Williams, *J. Chem. Soc., Chem. Commun.* **1987**, 1064-1066; c) P. R. Ashton, A. M. Z. Slawin, N. Spencer, J. F. Stoddart, D. J. Williams, *J. Chem. Soc., Chem. Commun.* **1987**, 1066-1069; d) M. Asakawa, P. R. Ashton, R. Ballardini, V. Balzani, M. Belohradsky, M. T. Gandolfi, O. Kocian, L. Prodi, F. M. Raymo, J. F. Stoddart, M. Venturi, *J. Am. Chem. Soc.* **1997**, *119*, 302-310; e) M. Asakawa, P. R. Ashton, S. E. Boyd, C. L. Brown, R. E. Gillard, O. Kocian, F. M. Raymo, J. F. Stoddart, M. S. Tolley, A. J. P. White, D. J. Williams, *J. Org. Chem.* **1997**, *62*, 26-37, and references therein; f) W. S. Bryant, J. W. Jones, P. E. Mason, I. A. Guzei, A. L. Rheingold, D. S. Nagvekar, H. W. Gibson, *Org. Lett.* **1999**, *1*, 1001-1004; g) J. W. Jones, L. N. Zakharov, A. L. Rheingold, H. W. Gibson, *J. Am. Chem. Soc.* **2002**, *124*, 13378-13379; h) Reviews: H. W. Gibson in *Large Ring Molecules* (Ed.: J. A. Semlyen), John Wiley & Sons, New York, **1996**, pp. 191-262; D. Philp, J. F. Stoddart, *Angew. Chem.* **1996**, *108*, 1242-1286; *Angew. Chem. Int. Ed. Engl.* **1996**, *35*, 1155-1196; A. Harada, *Acta Polym.* **1998**, *49*, 3; F. M. Raymo, J. F. Stoddart, *Chem. Rev.* **1999**, *99*, 1643-1664; E. Mahan, H. W. Gibson in *Cyclic Polymers, 2nd ed.* (Ed.: A. J. Semlyen), Kluwer Publishers, Dordrecht, **2000**, pp. 415-560.

2. a) S. J. Rowan, S. J. Cantrill, J. F. Stoddart, *Org. Lett.* **1999**, *1*, 129-132; b) F. Diederich, L. Echegoyen, M. Gomez-Lopez, R. Kessinger, J. F. Stoddart, *J. Chem. Soc., Perkin Trans. 2* **1999**, 1577-1586; c) T. Chang, A. M. Heiss, S. J. Cantrill, M. C. T. Fyfe, A. R. Pease, S. J. Rowan, J. F. Stoddart, A. J. P. White, D. J. Williams, *Org. Lett.* **2000**, *2*, 2947-2950; d) Reviews: M. C. T. Fyfe, J. F. Stoddart, *Adv. Supramol. Chem.* **1999**, *5*, 1-53; T. Takata, N. Kihara, *Rev. Heteroatom Chem.* **2000**, *22*, 197-218.
3. P. R. Ashton, S. J. Langford, N. Spencer, J. F. Stoddart, A. J. P. White, D. J. Williams, *J. Chem. Soc., Chem. Commun.* **1996**, 1387-1388.
4. a) S. J. Loeb, J. A. Wisner, *Angew. Chem.* **1998**, *110*, 3010-3013; *Angew. Chem. Int. Ed. Engl.* **1998**, *37*, 2838-2840; b) S. J. Loeb, J. A. Wisner, *J. Chem. Soc., Chem. Commun.* **1998**, 2757-2758; c) S. J. Loeb, J. A. Wisner, *J. Chem. Soc., Chem. Commun.* **2000**, 845-846; d) S. J. Loeb, J. A. Wisner, *J. Chem. Soc., Chem. Commun.* **2000**, 1939-1940; e) J. Tiburcio, J. E. G. Davidson, S. J. Loeb, *J. Chem. Soc., Chem. Commun.* **2002**, 1282-1283.
5. M.-V. Martínez-Díaz, N. Spencer, J. F. Stoddart, *Angew. Chem.* **1997**, *109*, 1991-1994; *Angew. Chem. Int. Ed. Engl.* **1997**, *36*, 1904-1907.
6. P. Job, *Ann. Chim.* **1928**, *9*, 113-203.
7. ¹H NMR characterizations were done on solutions with constant [3] and varied [4-2PF₆]. Based on these NMR data, $\Delta\delta$, the difference in δ values for protons of DB24C8 in the uncomplexed and fully complexed species, was calculated by using the Benesi-Hildebrand method (C. Gong, P. B. Balanda, H. W. Gibson, *Macromolecules* **1998**, *31*, 5278-5289). Then K_a was calculated from $K_a =$

$$(\Delta/\Delta_0)[\mathbf{3}]_o / \{ \{ [\mathbf{3}]_o - (\Delta/\Delta_0)[\mathbf{3}]_o \} \{ [\mathbf{4-2PF}_6]_o - (\Delta/\Delta_0)[\mathbf{3}]_o \} \}.$$

8. Errors were calculated by assuming $\pm 5\%$ error in Δ/Δ_0 . We found that apparent association constants K_a for some systems are concentration dependent so it is necessary to specify initial concentrations (Jones, J. W.; Gibson, H. W. *J. Am. Chem. Soc.* **2003**, *125*, 7001-7004; Huang, F.; Jones, J. W.; Gibson, H. W. accepted by *J. Am. Chem. Soc.*).
9. High resolution fast-atom bombardment mass spectrometry gave m/z 779.29187 (deviation 3 ppm).
10. X-ray data were collected on an Oxford Diffraction XCalibur2™ diffractometer equipped with the Enhance X-ray Source™ (MoK α radiation; $\lambda = 0.71073$ Å) and a Sapphire 2™ CCD detector. The data collection routine, unit cell refinement, data processing, the face-indexed numerical absorption correction were carried out with the program CrysAlis.¹¹ The Laue symmetry and systematic absences are consistent with the monoclinic space group *Pbcn*. The structure was solved by direct methods and refined using the SHELXTL NT program package.¹² One crown ether and half a paraquat-2PF₆ salt comprise the asymmetric unit. The final refinement involved an anisotropic model for all non-hydrogen atoms. A PF₆⁻ anions was modeled as being partially disordered over 2 positions, with each position constrained to 50% occupancy by symmetry. Idealized hydrogen atom positions and thermal parameters were calculated. Crystal Data: C₆₀H₇₈F₁₂N₂O₁₆P₂; FW 1373.18; T = 100.0 K; Orthorhombic *Pbcn*, $a = 13.3670(16)$ Å, $b = 29.614(3)$ Å, $c = 16.333(2)$ Å, $V = 6465.3(13)$ Å³; Z = 4; $\rho_c = 1.411\text{g}\cdot\text{cm}^{-3}$; $\mu = 0.169\text{ mm}^{-1}$; F(000) = 2872; crystal dimensions: 0.50 x 0.15 x

0.06 mm³; θ range = 2.85 to 23.08°; index ranges: $-14 \leq h \leq 14$, $-32 \leq k \leq 32$, $-17 \leq l \leq 17$; reflections: 34029, 4532 independent [R(int) = 0.0533]; numerical absorption correction (95.0-98.9% transmission); 4532 data / 435 parameters; R1 = 0.1628 (I > 2 σ); wR2 = (all data); 0.3311; goodness of fit (F²) = 1.131; max and min residual electron density = 0.892 and -0.553 e.Å⁻³. CCDC-201689 contains the supplementary crystallographic data for this paper. These data can be obtained free of charge via www.ccdc.cam.ac.uk/conts/retrieving.html (or from the Cambridge Crystallographic Data Centre, 12, Union Road, Cambridge CB2 1EZ, UK; fax: (+44) 1223-336-033; or deposit@ccdc.cam.ac.uk).

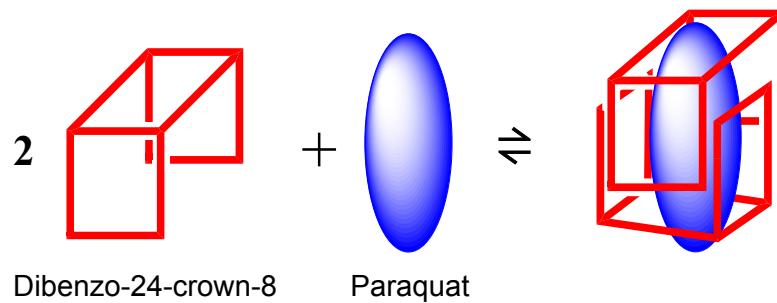
11. Oxford Diffraction, Wroclaw, Poland, **2002**.
12. G. M. Sheldrick, SHELXTL NT ver. 6.12; Bruker Analytical X-ray Systems, Inc.: Madison, WI, **2001**.
13. M. M. Conn, J. Rebek, Jr., *Chem. Rev.* **1997**, *97*, 1647-1668; A. Jasat, J. C. Sherman, *Chem. Rev.* **1999**, *99*, 931-967; Z. Zhong, A. Ikeda, M. Ayabe, S. Shinkai, S. Sakamoto, K. Yamaguchi, *J. Org. Chem.* **2001**, *66*, 1002-1008; F. Hof, S. L. Craig, C. Nuckolls, J. Rebek, Jr., *Angew. Chem.* **2002**, *114*, 1556-1578; *Angew. Chem. Int. Ed. Engl.* **2002**, *41*, 1488-1508; J. Chen, J. Rebek, Jr., *Org. Lett.* **2002**, *4*, 327-329; M. R. Johnston, M. J. Latter, R. N. Warrener, *Org. Lett.* **2002**, *4*, 2165-2168; F. Corbellini, R. Fiammengo, P. Timmerman, M. Crego-Calama, K. Versluis, A. J. R. Heck, I. Luyten, D. N. Reinhoudt, *J. Am. Chem. Soc.* **2002**, *124*, 6569-6575; J. L. Atwood, L. J. Barbour, A. Jerga, *Proced. Natl. Acad. Sci. U. S. A.* **2002**, *99*, 4837-4841; R. Zadnani, T. Schrader, T. Grawe, A. Kraft, *Org. Lett.* **2002**, *4*, 1687-1690; R. Mungaroo, J. C. Sherman, *J. Chem. Soc.*,

Chem. Commun. **2002**, 1672-1673.

14. X-diffraction was carried out on Bruker Apex CCD diffractometer equipped with MoK α radiation ($\lambda = 0.71073 \text{ \AA}$) and a graphite monochromator. Data were collected from $\theta = 2.38^\circ$ to $\theta = 24.99^\circ$ by using phi and omega scans. Crystal data: rod, colorless, $0.50 \times 0.10 \times 0.10 \text{ mm}$, $C_{75}H_{98}F_{12}N_2O_{25}P_2$, FW 476.19, orthorhombic, space group *Pnma*, $a = 14.4612(16)$, $b = 11.6741(13)$, $c = 10.6275(11) \text{ \AA}$, $\alpha = 90^\circ$, $\beta = 90^\circ$, $\gamma = 90^\circ$, $V = 1794.2(3) \text{ \AA}^3$, $Z = 4$, $D_c = 1.763 \text{ g cm}^{-3}$, $T = 218 \text{ K}$, $\mu = 3.62 \text{ cm}^{-1}$, 10268 measured reflections, 1664 independent reflections, 139 parameters, $F(000) = 752$, $R1 = 0.0757$, $wR2 = 0.1816$ (all data), $R1 = 0.0674$, $wR2 = 0.1753$ [$I > 2\sigma(I)$], max. residual density $0.498 \text{ e} \cdot \text{\AA}^{-3}$, max./min. transmission $0.9647/0.8397$, and goodness-of-fit (F^2) = 1.113. The structure was solved by SHELXS-97^[15] and refined by SHELXL-97.^[16] Nonhydrogen atoms were treated anisotropically and hydrogen atoms were placed in calculated positions. 1664 reflections were used in refinements by full-matrix least-squares on F^2 . CCDC- 201688 contains the supplementary crystallographic data for this paper. These data can be obtained free of charge via www.ccdc.cam.ac.uk/conts/retrieving.html (or from the Cambridge Crystallographic Data Centre, 12, Union Road, Cambridge CB2 1EZ, UK; fax: (+44) 1223-336-033; or deposit@ccdc.cam.ac.uk).
15. G. M. Sheldrick, SHELXS-97, Program for the Solution of Crystal Structures, University of Göttingen, Göttingen (Germany), **1997**.
16. G. M. Sheldrick, SHELXL-97, Program for the Refinement of Crystal Structures, University of Göttingen, Göttingen (Germany), **1997**.

17. High resolution fast-atom bombardment mass spectrometry gave m/z 839.30872 (deviation 2.3 ppm).
18. Hansch, C.; Leo, A.; Taft, R. W. *Chem. Rev.* **1991**, *91*, 165-195.
19. N-(2-Hydroxyethyl)-N'-methyl-4,4'-bipyridinium bromide iodide was reported before (Tundo, P.; Kippenberger, D. J.; Politi, M. J.; Klahn, P.; Fendler, J. H. *J. Am. Chem. Soc.* **1982**, *104*, 5352-5358). The same method was used to prepare this compound and then ion-exchanging to PF₆ counterions was applied by using aqueous ammonium hexafluorophosphate. The crude product was purified by recrystallization from water three times to provide pure **8a**-2PF₆ as white crystals. mp 240.5-241.6 °C. ¹H NMR (400 MHz, acetone-*d*₆, 22 °C) δ(ppm): 9.47 (m, 4H), 8.92 (d, *J* = 7.3 Hz, 4H), 5.11 (t, *J* = 5.0 Hz, 2H), 4.80 (s, 3H), 4.73 (t, *J* = 5.0 Hz, 1H), 4.26 (m, 2H). Anal. calcd for C₁₃H₁₆N₂O₁P₂F₁₂: C, 30.83; H, 3.19; N, 5.53. Found: C, 30.94; H, 3.15; N, 5.54.
20. Ashton, P. R.; Philp, D.; Reddington, M. V.; Slawin, A. M. Z.; Spencer, N.; Stoddart, J. F.; Williams, D. J. *Chem. Commun.* **1991**, 1680-1683.
21. Wolfle, I.; Lodaya, J.; Sauerwein, B.; Schuster, G. B. *J. Am. Chem. Soc.* **1992**, *114*, 9304-9309.
22. Shen, Y. X.; Engen, P. T.; Berg, M. A. G.; Merola, J. S.; Gibson, H. W. *Macromolecules* **1992**, *25*, 2786-2788.

TOC Graphic:



Abstract: Some new [2]pseudorotaxanes based on the dibenzo-24-crown-8/paraquat recognition motif were prepared. They were characterized by ^1H NMR, mass spectrometry, and X-ray analysis.
